Bulletin of the Czech Geological Survey, Vol. 77, No. 2, 127–134, 2002

Investigation of granite inhomogeneity with well logging methods

LÁSZLÓ ZILAHI-SEBESS[1] – GÁBOR SZONGOTH[2]

[1]Eötvös Loránd Geophysical Institute of Hungary, Kolumbusz utca 17-23., H-1145 Budapest, Hungary
[2]Geo-Log Environmental and Geophysical Ltd., Rákospatak utca 79/b., H-1142 Budapest, Hungary; e-mail: posta@geo-log.hu; tel/fax: ++36 1 3635643

Abstract. In this study we present a case history on the investigation of a fissure-system in granite rock of the Krušné hory Mts., Czech Republic, with the help of well logging methods. We applied acoustic borehole televiewer (BHTV) as the most important tool, but we made several additional logs, too, which are very sensitive to the fractures (full wave sonic, resistivity, caliper). The real influx points from among the open fissures were detected with heat pulse flowmeter (HPF) logging. This paper provides information obtained from BHTV measurements and the integrated interpretation of logs. Some statements were made on the geotechnical state of the granite body.

Key words: granite, tectonic control, fracture, fracturing, flow mechanisms, well-logging, acoustic borehole televiewer, heat pulse flowmeter

Introduction

Our company – Geo-Log Environmental and Geophysical Ltd.– was requested to perform borehole televiewer (BHTV) logging in the PTP-3 borehole. The objective of the investigation was to examine the fissure-system in a granite rock of the Podlesí stock in Krušné hory Mts. (Breiter 2002). The acoustic borehole televiewer logs were necessary to find the real direction of core-scanner data (Maros et al. 2002), but we also carried out the independent interpretation of the logs (fissure location, direction, statistical calculations). Logging was made in two phases down to 348 m depth.

We had preliminary experience neither on the geological structure, nor on the geotechnical state of the territory; that is why we had to record some additional logs besides the BHTV measurement. We measured caliper-log to examine the technical state of the borehole; full-wave sonic and resistivity logs (10 cm and 40 cm), because these are the most sensitive to the alteration of the fresh granite. There is no influx at all open fissures, therefore to detect the real influx zones we measured Heat Pulse Flowmeter (HPF) log in the upper section of the borehole.

The following tools were used for logging:
Acoustic BoreHole TeleViewer: ALT (Luxembourg) type FAC-40A;
Caliper, Temperature, Sonic Waveform: ELGI (Hungary);
Heat Pulse Flowmeter: Mount Sopris (USA) type HPF-4293.

BHTV measurement

Acoustic borehole televiewer measurement, which outside the oil industry is considered new method in Hungary, allows high resolution, *in situ* study of the fissure-system. With the borehole televiewer the travel time and amplitude of the signal generated by a rotating sonar (sonic transmitter) is recorded in minimum 72, maximum 288 directions.

Plotting the result with a colour code the image of borehole wall is obtained, laid out in a plane. Only the fractures open from acoustic viewpoint can be recognized in the image constructed from the reflections' travel times. All those forms, which have elastic parameters different from their surroundings, can be seen in the image constructed from the amplitudes of reflections; thus the filled fractures as well.

Possibility for fracture aperture determination

In spite of the fact that on the BHTV record the open and closed fractures may be distinguished, measurement of the true fracture aperture is difficult. For a 1 MHz transmitter frequency the tool's resolution is about 1mm, but the depth sampling rate at 1 m/min logging speed, is 4 mm; thus the 1 mm resolution is valid for linear objects only.

On the other hand fissures thinner than 1 mm can be detectable on the amplitude image, because there is frequently a mechanically damaged zone around the fissure, in connection with the forces that caused it. Amplitudes of the acoustic waves reflected from damaged zone are smaller than from the fresh part of the rock; it means that the apparent width of the fissures seems to be wider than the resolution of the BHTV tool. Generally, there is no change in travel time from the damaged zone without void, therefore such kind of fissures cannot be seen on the reflection image, independently of the quality of the fissure.

Expectedly, the order of apparent fissure aperture is approximately the same as that of the real one; in other words, apparent fracture aperture is in close connection with the real one. There is low probability for getting information on fracture aperture for wide fractures, because along the wide fractures the core may fall into pieces, therefore in most cases it is not measurable.

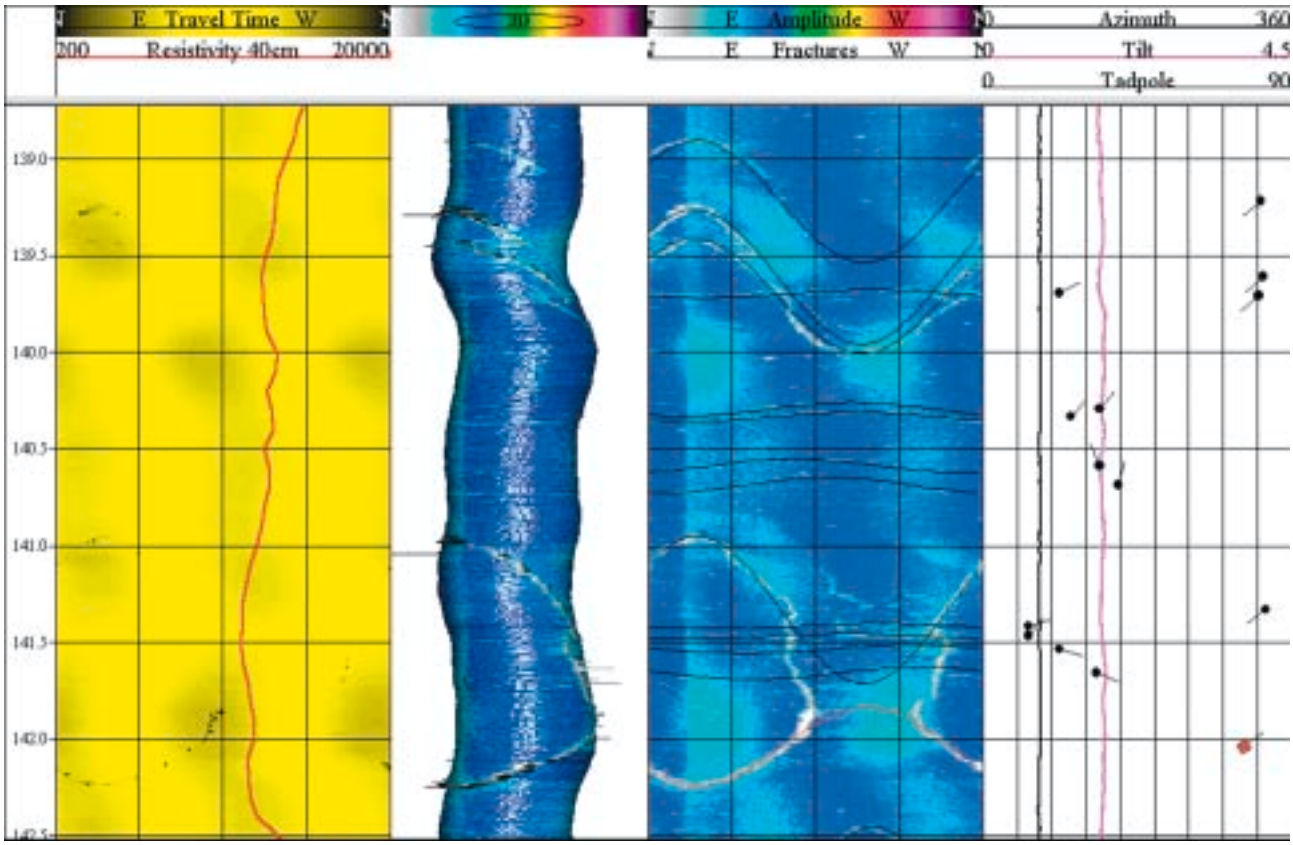

Fig. 1. Separation of open and closed fissures based on the borehole televiewer measurement.

BHTV evaluation

The acoustic borehole televiewer measurement was carried out from 19 m down to 348 m. During the evaluation, we selected 1085 fractures based on the total of 329 m measurements. During the classification of the fractures – from acoustic point of view – those of them are considered open which can be seen in the travel time image as well.

Indications of fractures have been categorized as follows:
Open fracture (a complete sinus can be fitted to it) – red dot;
Partly open fracture (yielding an incomplete sinus) – violet dot;
Distorted open fracture (it does not yield a complete sinus or a sinus can imperfectly fit into it), this category contains all fractures which can be characterized by not a single plane – red square sign;
Closed fracture (all indications of fracture which cannot be seen in the travel time image) – black dot;
Distorted closed fracture (yielding an incomplete sinus or a sinus can imperfectly fittinto it) – black square sign.

Only those fissured zones are considered real fracture zones where a large number of open fissures can be seen on the borehole televiewer reflection time image.

In general, the amplitude image is richer in details, the fissures closed from acoustic viewpoint appear only on this image (Fig. 1, the white sinusoids between 139.0–141.5 m). A larger, single open fissure appears in the travel time image as black sinusoid at 142.0 m.

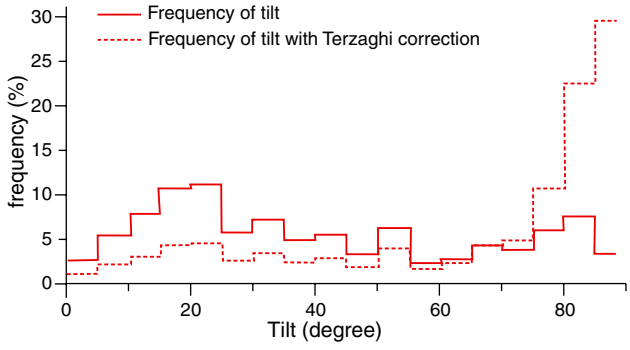

Fig. 2. Distribution of tilt angles.

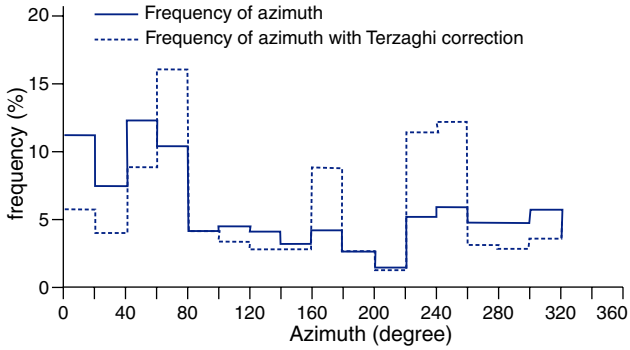

Fig. 3. Distribution of tilt azimuths.

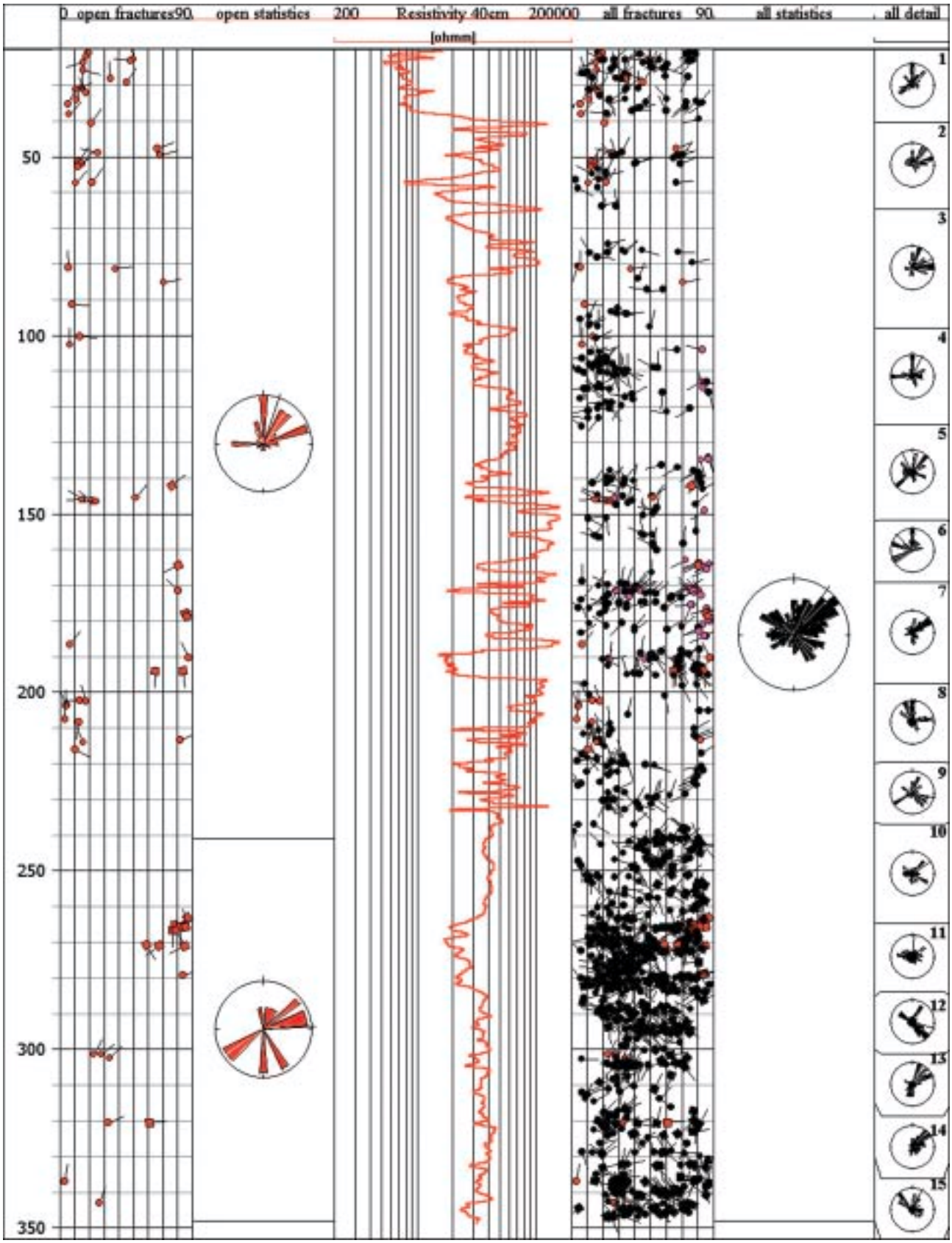

Fig. 4. Resistivity, fracture markings and their statistics (without Terzaghi correction).

Dip distribution can be seen in Fig. 2; without correction dips about 20–25° are the most frequent, but steep dips have also a definite frequency maximum around 75–85°. After the Terzaghi correction, the nearly vertical fractures are unambiguously the most frequent ones. (With the Terzaghi correction we take into consideration that the projection of a given

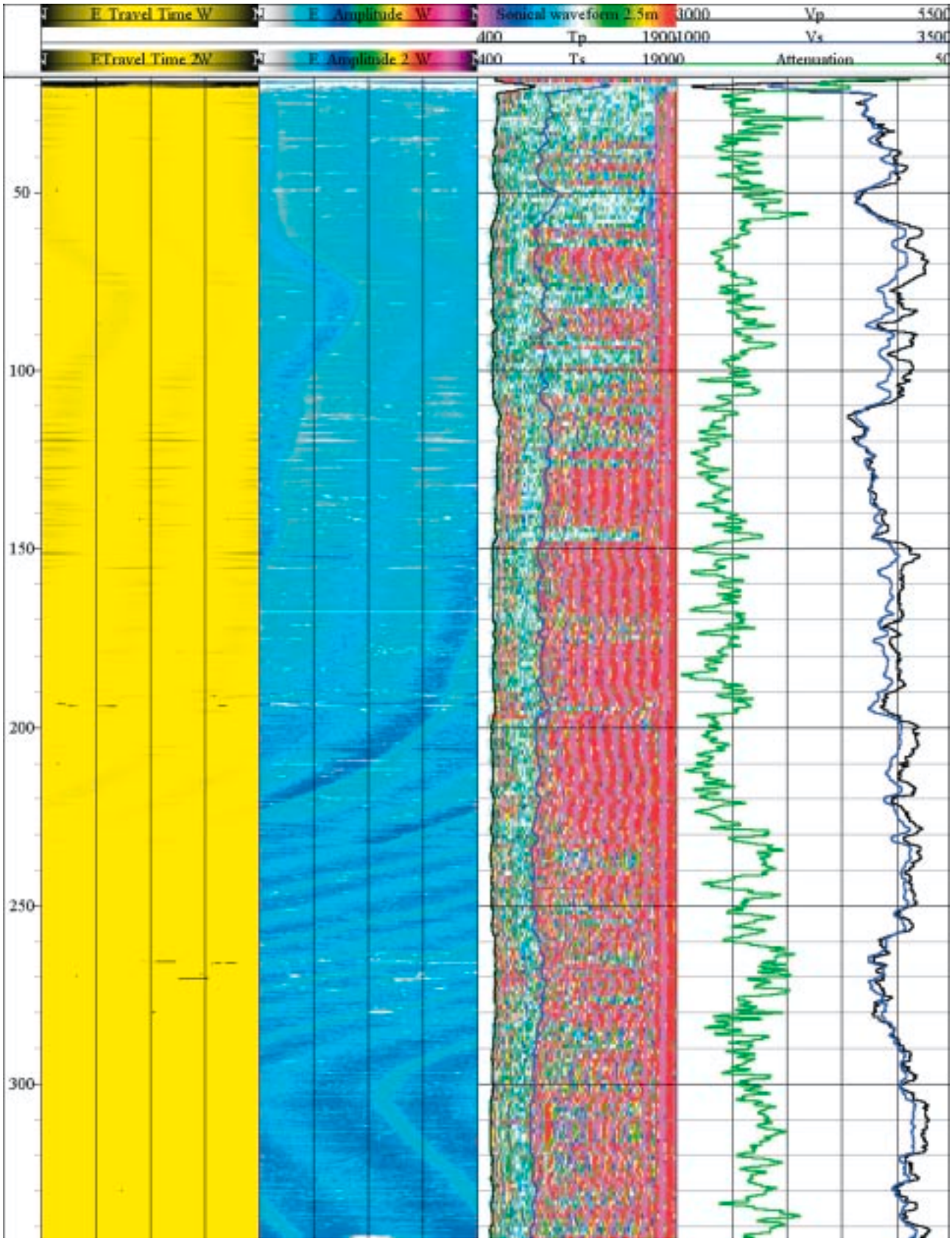

Fig. 5. BHTV measurement and fracture marking, and complementary geophysical measurements.

real fracture density depends on the dip angle of the fracture system. This correction means a multiplication by the weight factor, where α is the dip angle).

Statistics of dip directions is shown in Fig. 3. Without correction the most frequent direction falls into the 40-60° interval and the frequency of directions around 120°–140° and

300°–320° is also dominant. After correction the two most frequent dip directions are: 60–80°, 240–260° (there are other frequent directions as well: 160–180°, 100–120° and 300–320°). Thus, the major strike direction of fractures is (150–170°) – (330–350°), i.e. SSE-NNW from the corrected data set.

The open fractures are shown in the traditional tadpole representation in the first column of Fig. 4. Rose diagram of the open fractures is plotted in the second column of Fig. 4. The most frequent direction of open fractures is NE down to the depth of 240 m; this is because of the small number of data means practically scattered data in the NE sector. Below 240 m the small number of the open fractures have E-NE, SSE and SW orientation.

Based on the acoustic waveform, the electric resistivity logs and the fractures marked out, the borehole has been divided into the 15 intervals.

In the last column the distribution of dip directions within the individual intervals is shown without correction. The most frequent directions vary from interval to interval; one of the three major directions characterizing the whole borehole according to the rose diagram (40–60°, 120–140° and 300–320°, which otherwise correspond to the uncorrected histogram) appear most definitely in intervals 1, 2, 5, 6, 7, 9, 10, 11, 12, 13, 14 and 15.

It can also be stated that the direction between 160 and 180° without correction appears in interval 7 only as a secondary direction. Terzaghi correction enhanced this direction only because there is a high number of extremely steep dips of this direction in interval 7, in other words its projection to the whole borehole are not reasonable, because it characterizes only one interval.

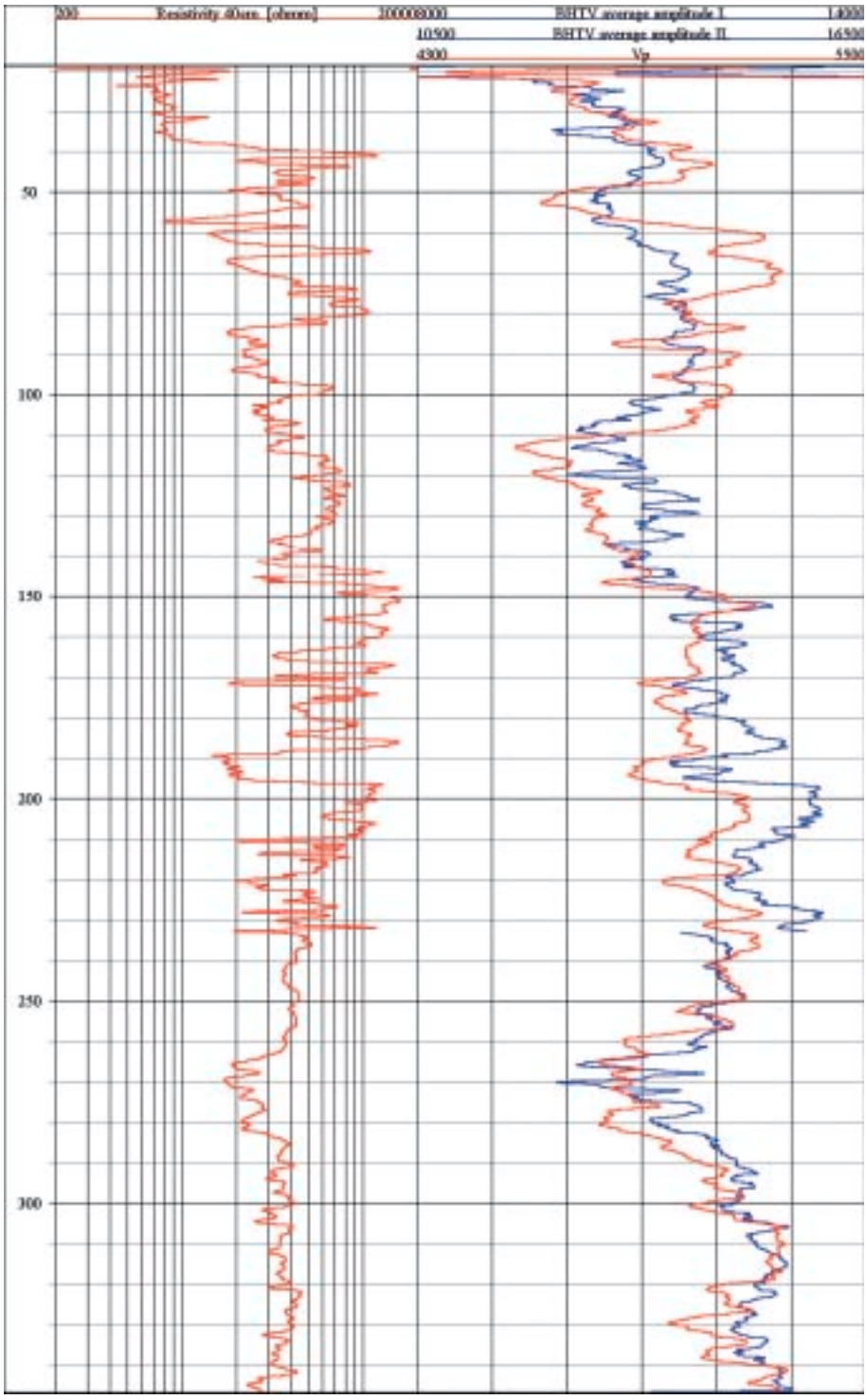

Fig. 6. Correlation between the resistivity, wave velocity and BHTV amplitude.

Based on the measurements it can be stated that the distorted, open fractures occur mainly below 135 m, and also that the proportion of steep (70°) fractures increases with depth. The proportion of distorted, closed fractures is the highest in the section below 240 m.

Summarizing, it can be stated that in this borehole the detectable fracture density down to a depth of 240 m is only 10–20% of that experienced in Hungarian granite (Zilahi-Sebess 2000), thus, this rock is very compact. In the interval between 240 and 348 m the fracture density relatively increases, but majority of it represents distorted, closed fractures, in other words they are supposedly inactive from hydrogeological point of view. Interval 11 (264.8–284.9 m) contains a great part of the open fractures in the section below 240 m, and 22% of all fractures in the whole borehole.

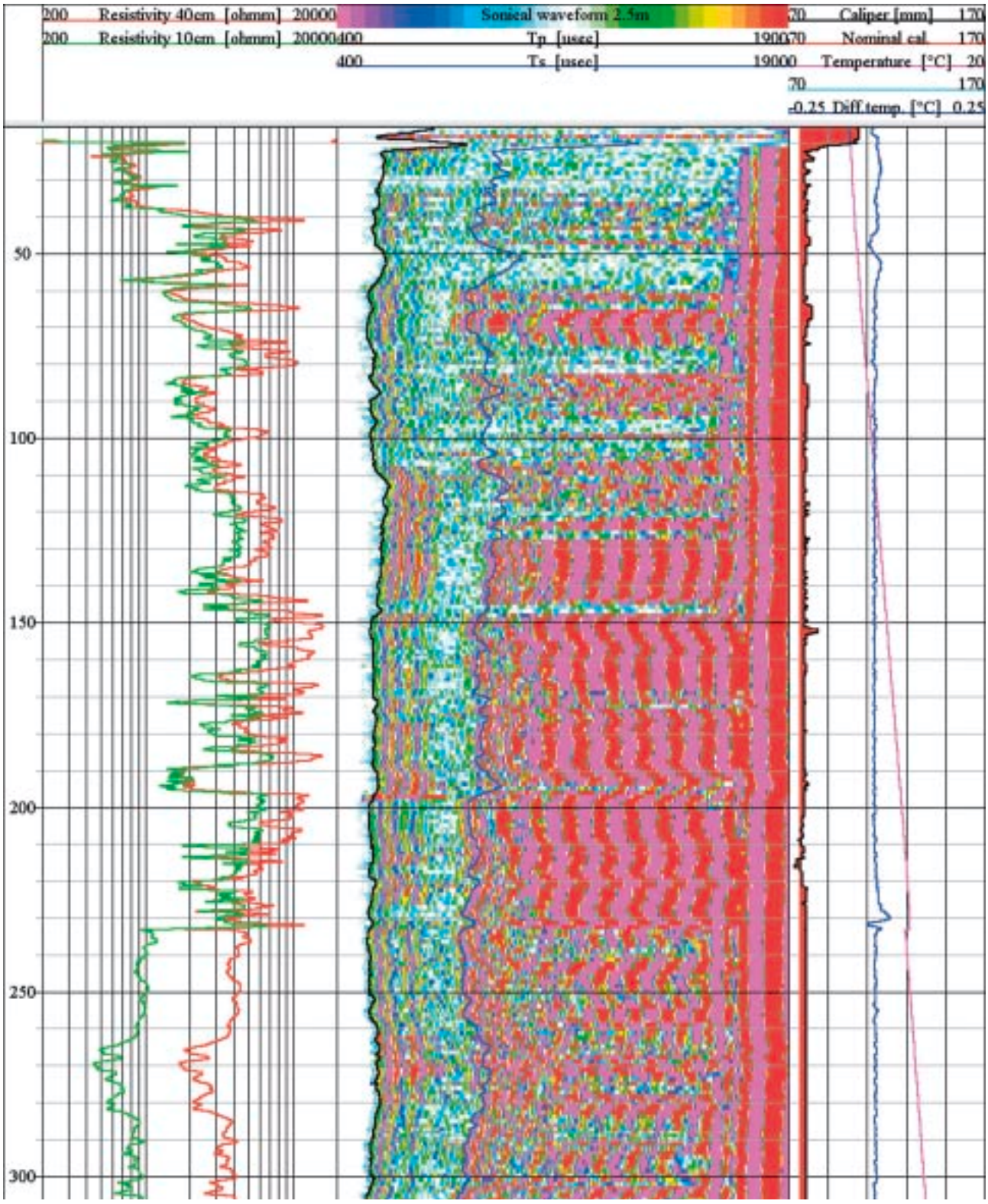

Fig. 7. Resistivity, acoustic waveform and technical measurements.

Integrated interpretation based on BHTV and other measurements

In addition to the ordered BHTV measurement we carried out the following measurements in the borehole: caliper, temperature, SP, electrical resistivity with 10 and 40 cm long potential tools and acoustic waveform. Assessment of the borehole technical conditions and the geotechnical condition justified completion of these measurements. Decreases in amplitude of acoustic waveform correlate well with the fractures detected with the BHTV down to 126.5 m, below this only the more intensively fractured zones can be correlated (Fig. 5).

According to the amplitudes of waveform the rock

seems to be more weathered than expected from the relatively high velocity. The propagation velocity (V) is nowhere less than 4 500 m/s; this means a porosity of maximum 5%. It is very likely that a small number of thin fractures representing a very small total porosity reduces the acoustic velocity only slightly.

The transversal wave arrival has also been marked out in the acoustic waveform; based on this the value of V_P/V_S is about 1.7–1.75. The attenuation log was defined as the attenuation of longitudinal wave packets measured with two different tool lengths for the four periods after the first break. (Further rock mechanical parameters can also be calculated if the density log is also available.)

The amplitude image of the acoustic borehole televiewer or a part of it – an amplitude log recorded along some generatrices – has been transformed into a continuous log. The averaged amplitude log obtained this way characterizes the seismic hardness of the rock and its mechanical state. It can be seen in Fig. 6 that the geotechnical condition of rock improves more intensively with depth, down to about 200 m; this is in conformity with trend-like changes observed in acoustic velocity and resistivity logs as well. This phenomenon is analogous with our experience gained on the weathered zone of Hungarian Mórágy Granite (Zilahi-Sebess et al. 2000). The difference between the weathered zone of granites in PTP-3 borehole and Mórágy is that in Podlesí are high velocities very near to the surface. Our conclusion is that this weathered zone may be analogous only to the bottom part of the weathered crust of the Mórágy Granite; this may be in connection with decreasing acoustic attenuation caused rather by unloading than real surface weathering.

Below 200 m – primarily due to the more intensively fractured zone between 265 and 285 m (interval 11) and its vicinity – this trend does not continue.

Based on the BHTV average amplitude, number of fractures and acoustic wave propagation velocity intervals between 47 to 59 m, 105 to 125 m and 265 to 285 m are considered the loosest ones; on the other hand, based on the acoustic velocities higher than 4 500 m/s they can be considered also hard, unweathered, solid rock.

Electrical resistivity logs do not correlate with the acoustic waveform in the usual way; a decrease in electrical resistivity does not belong to each decrease in acoustic velocity (Fig. 7). E.g., at the local low resistivity, between 66.0 and 73.5 m, there are high amplitudes in the acoustic waveform, and the acoustic velocity is high as well. Comparison with the BHTV measurement demonstrates, that not the fracturing causes the decrease in resistivity in this interval. It can be assumed that the conductivity of the rock matrix is somewhat higher; this may be caused by a small increase in clay content, or by low ore concentration. Along fissures and microcraks the minerals may partly turn into clay minerals.

Considering the resistivity of the rock-forming minerals around 10^9 Ωm, practically they are isolators; 1 ppm conductive material with 10^{-3} Ωm resistivity may decrease the true resistivity down to 1 000 Ωm, if the conductive minerals are in connection with each other. We suppose that this condition is realistic, because forming of ore grains regularly is in close connection with forming of fissure system of rock.

According to some simplified calculations on resistivity, 0.5% clay mineral content is approximately equivalent to 5 Ωm resistivity. In this case the measurable resistivity with 10 Ωm mud resistivity is nearly the same (around 900 Ωm) as the true 1 000 Ωm resistivity, while the measurable resistivity for 10^9 Ωm true resistivity of absolutely non-altered rock is 10^4 Ωm only.

According to the above the values of resistivity minimum measured with the 40 cm long tool are around 2 000–3 000 Ωm, therefore only a very weak effect (ore concentration) could be considered; this – assuming the 10^{-3} – 10^{-4} Ωm resistivity of sulfide ores – can also be caused by a concentration of 1–0.1 ppm.

The dynamic range of resistivity measurement decreased in the section of the second measurement (below 233 m) due to the effect of the applied low resistivity mud. The more intensively fractured interval 11 between 265–285 m is unambiguously of low resistivity compared to its vicinity. Apart from the absolute value of resistivity, under 230 m in stock granite the apparent stratification (frequency of changes versus depth) is less visible than in the biotite granite. In the full waveform acoustic record (Fig. 7) under 230 m it can be seen that the amplitudes of waves decreased (lighter colors on the picture) in comparison to the amplitudes in biotite granite.

Interpretation of the HPF measurement

At first, measurements were carried out in the stationary well (see Fig. 8), and we detected a slight downward flow down to 40 m. The likely reason for that is that the cavern below the rotary shoe swallows (about 0.2 l/min) bulk of the water dropping down alongside the pipe, and the remaining 0.1 l/min water is swallowed down to 40 m.

The depression was generated with our own pump, the diameter of the pump was 3”. Because of the well’s structure we could lower the pump only down to about 22 m. Prior to the measurement (the stationary water level was –11.1 m) we had attempted to set the maximum depression for a few hours. Initially, we produced about 4 l/min of water, but the water level rapidly sunk. After that, a part of the water was led back to the well, in this way we succeeded in setting an approximately stable water level (at –20.5 m).

Tab. 1. According to the HPF measurement inflow was experienced at the following intervals.

Number of interval	Depth interval (m-m)	Major fracture direction	Measured inflow (l/m)
I	26–28	N, NNE, SSW	0.5
II	31–32		0.2
III	36–38		0.2
IV	38–39	WSW (219°–257°)	0.8
V	41–42		0.2
VI	48.5–51	ENE (73°)	1.3
VII	77–79		0.1

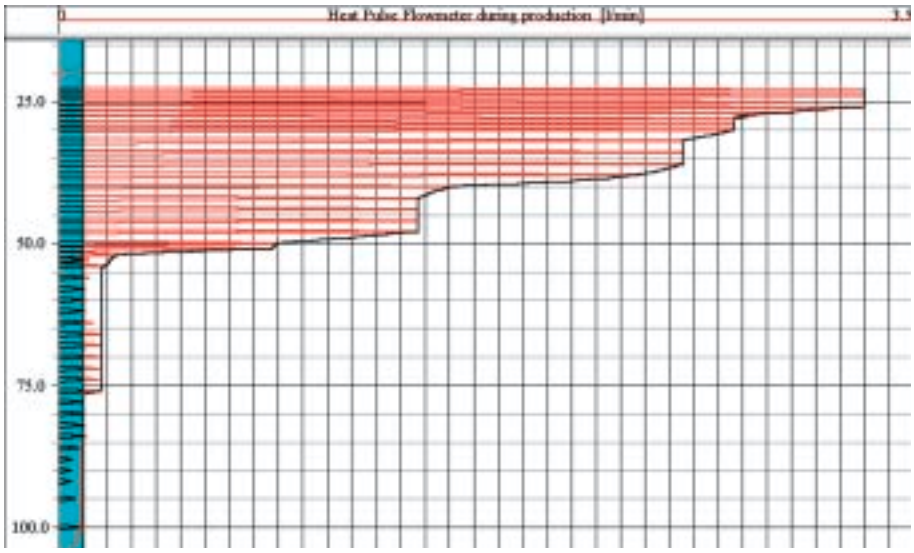

Fig. 8. Flowmetry with high sensitive flowmeter during production.
The blue strip means the absolute error of the tool around zero. The accuracy of the tool is ±0.1 l/min.

With the progress of time production had to be reduced, to maintain the dynamic water level; at the end the production was only 1.5 l/min; this means that the water supply was extremely weak.

From the measurement shown in Fig. 8 can be stated that there is no significant water inflow below 52 m at this depression (–9.4 m)! Production from the lower layers would be possible only if depressions were increased, because their stationary water level is obviously below –20.5 m. A multiple-stage pump of 2" would be required for that, or the upper part of the well should be reamed to a diameter of 100 mm at least down to 50 m. If this is feasible, the measurement can be continued down to the bottom and each layer can be tested. With few days continuous measurement the stationary water level (pressure) belonging to each layer can be determined.

Places of inflow correlate better with places of decrease or increase in V_p, or changes in BHTV average amplitude, than with interior of more intensively fractured zones and generally are associated with places where steep fractures exist.

Each of zones I, IV and VI can be found in such a position where instead of or in addition to the flat fractures, fractures steeper than 60° also appear. The most intensive inflow was observed at interval VI, where the average direction of fractures is 73° (ENE), which coincides with the most frequent direction after the Terzaghi correction.

Conclusions

The methods that are the most sensitive to fractures are based on electrical and acoustic principles. Fractures cause electrical resistivity to drop, however, minimal ore or clay mineral content in connection with non-detectable microcracks can also reduce resistivity. In the acoustic waveform the more significant fracture intervals appear with reduced amplitude, their first arrival is later than that of the intact rock, and generally the shear wave propagation time significantly increases. For the direct indication of individual fractures, to separate open and closed fractures appearing on the borehole wall, and to determine the direction of the fractures, the most suitable geophysical method is the acoustic borehole televiewer. There is no inflow at each of the open fractures; we use the heat pulse flowmeter measurement to determine this.

Only qualitative correlation can be obtained between the fracture density, determined from the measurements (fracture/m), and electrical resistivity. The main reason for this is that the investigated rock may have a low ore content (1–0.1 ppm), which reduces resistivity even where fracture density is low. Based on Fig. 7 (electrical resistivity, acoustic waveform) the weathered crust of the granite extends to approximately 150 m. Considering the whole volume of granite, most common are the fissures with tilts steeper than 70°, while the rarest are those under 15°. The number of fractures found in the borehole above 240 m is very low, below that it increases, but the number of open fractures is still low. The interval 264.8–284.9 m contains the majority of the open fractures that can be found below 240 m; this can be considered as the main water-conducting zone. Contrary to this, based on the HPF measurements, there is no significant inflow at 20.5 m depression, below 52 m.

References

Breiter K. (2002): From explosive breccia to unidirectional solidification textures: magmatic evolution of a phosphorus- and fluorine-rich granite system (Podlesí, Krušné hory Mts., Czech Republic), Bull. Czech Geol. Surv. 77, 2, 67–92.

Broding R. A. (1982): Volumetric scanning well logging: The Log Analyst, 23, 1, 14–19.

Faraguna J. K., Chace D. M., Schmidt M. G. (1989): An improved borehole televiewer system: image acquisition, analysis and integration: Society of Professional Well Log Analysts Annual Logging Symposium, 30th, Denver, Colo., 1989, Transactions, paper UU.

Georgi D. T. (1985): Geometrical aspects of borehole televiewer images: Society of Professional Well Log Analysts Annual Logging Symposium, 27th, Dallas, Tex., 1985, Transactions, 1–C.

Maros Gy., Palotás K., Koroknay B., Sallay E. (2002): Tectonic evaluation of borehole PTP-3 in the Krušné hory Mts. with ImaGeo mobile corescanner. Bull. Czech Geol. Surv. 77, 2, 105–112.

Zemanek J., Glenn E. E., Norton L. J., Caldwell R. L. (1970): Formation evaluation by inspection with the borehole televiewer. Geophysics, 35, 254–269.

Zilahi-Sebess L., Mészáros F., Szongoth G. (2000): Characterization of fracture zones in granite, based on well-logging data at the Üveghuta site. Annual report of the Geological Institute of Hungary 1999, 253–266

Zilahi-Sebess L., Rigler Gy., Szongoth G. (2000): Division of the weathering crust of the Üveghuta granite based on well-logging data. Annual report of the Geological Institute of Hungary 1999, 213–224.